SYSTEM MODELING AND ANALYSIS TOOLS

Contents

1.1 Introduction

A wind turbine is mainly composed by rotor, blades, tower and nacelle including gear box and generator, as shown in Figure 1.1; for the floating one, there is an additional floating platform. The principle of energy conversion applied to wind systems is that the kinetic energy of the wind is received by the blades and forces the rotor to rotate. Then, the kinetic energy is transferred into mechanical energy; in the nacelle, the low speed shaft (LSS) rotates with the rotor and is connected to a generator with the high speed shaft (HSS) via a gear box. Then, the mechanical power is transferred into electric energy.

This chapter describes the modeling of a FWT system and the simulation environment. The first section introduces the physical model of the FWT, including the coordinates system, the power

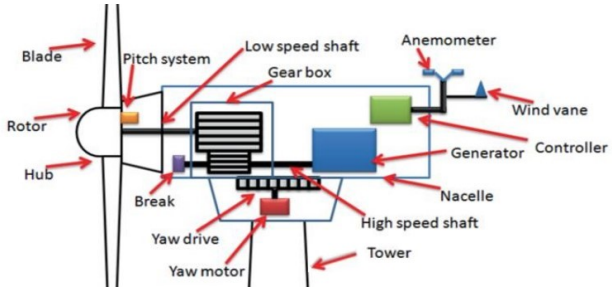

Figure 1.1 – Components of a wind turbine (Karimirad 2014).

capture system [1], the drive train system and a brief explanation of hydrodynamics of the floating structure. The second part describes the linearized model of the FWT system, for the purpose of control design; a reduced linear model is introduced and compared with FAST nonlinear model. The last part presents the analysis tools, the FWT under interest in this work, and the performance indicators used in this work.

1.2 Physical model

This section is devoted to the description of the models of the FWT elements. The coordinate system, power capture system, drive train system and the hydrodynamics of FWTs are introduced.

1.2.1 Coordinate systems

Figure 1.2 displays the 6 DOFs of motions of a floating platform. There are the platform surge, sway and heave translations and the platform roll, pitch and yaw rotations.

The platform surge translation is along with the x_p-axis (pointing horizontally in the downwind direction); the platform sway translation is along with the y_p-axis (perpendicular to the x_p-axis in the horizontal direction, pointing to right when looking face to the wind). Finally, the platform heave translation is along with the z_p-axis (pointing vertically upward opposite to gravity). When the platform is rolling, it rotates about the x_p-axis; when the platform is pitching, it rotates about the y_p-axis; when the platform is yawing, it rotates about the z_p-axis (Jason M Jonkman, M. L. Buhl Jr, et al. 2005).

Tower base coordinate system is shown in Figure 1.3. Its origin is located in the center of the intersection of tower base and platform: x_t-axis pointing horizontally in the opposite of upwind direction;

1. In this chapter, only the mechanical part of power capture system is discussed; the electrical part will be detailed in the next chapter.

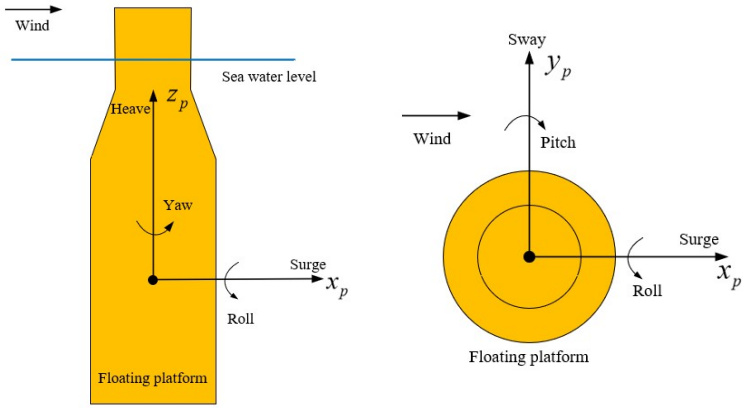

Figure 1.2 – Floating platform coordinate system. **Left.** Front view. **Right.** Top view.

y_t-axis being perpendicular to the x_t-axis in the horizontal direction, pointing to right when looking face to the wind. Finally, z_t-axis is pointing vertically up from the tower base.

In this coordinates system, tower base fore-aft, side-to-side and torsional moments are defined. Tower base fore-aft moment is caused by the tower pitching about the y_t-axis; tower base side-to-side moment is caused by the tower rolling about the x_t-axis; tower base torsional moment is caused by the tower yawing about the z_t-axis (Jason M Jonkman, M. L. Buhl Jr, et al. 2005).

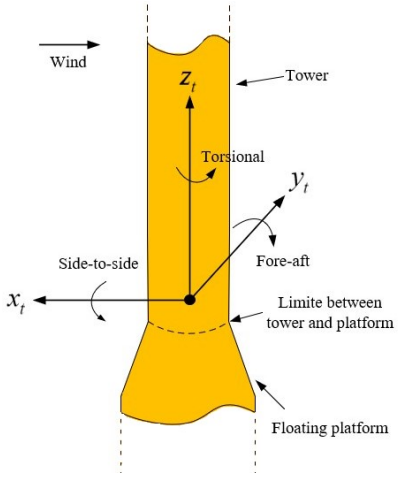

Figure 1.3 – Tower base coordinate system.

Blade coordinates system is shown in Figure 1.4-left. x_{bi}-axis ($i = \{1,\ 2,\ 3\}$ for blade 1, 2 or 3 respectively) is pointing horizontally to the nacelle from the center of the blade root; z_{bi}-axis is

pointing along the pitch axis towards the tip of blade i; y_{bi}-axis is parallel with the chord line (see Figure 1.4-right), pointing to the trailing edge (see Figure 1.4-right).

The blade flap-wise moment is caused by the flap-wise force about the y_{bi}-axis at the blade root; the blade edge-wise moment is caused by the edge-wise force about the x_{bi}-axis at the blade root.

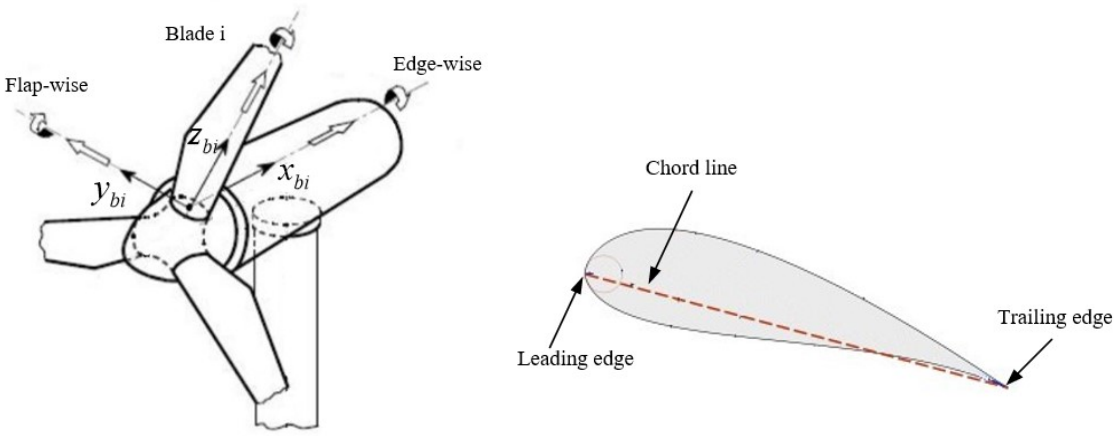

Figure 1.4 – **Left.** Blade coordinates system, adapted from (Jelavić, Petrović, and Perić 2010). **Right.** Blade section.

Finally, the rotor azimuth angle ψ is defined between the vertical axis and the current position of the blade #1 symmetrical axis (see Figure 1.5).

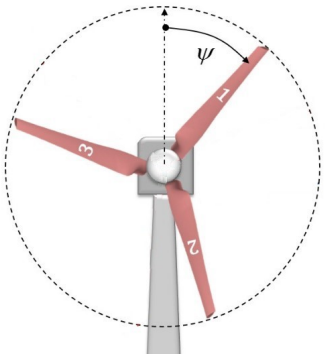

Figure 1.5 – Rotor azimuth angle (Cheon et al. 2019).

1.2.2 Power capture system

The turbine captures energy from the wind passing through its blades and transforms it into mechanical energy. Assume that the wind turbine is facing the wind; then, the mechanical power can be expressed as (Huang, F. Li, and Jin 2015; Guenoune et al. 2017; Yenduri and Sensarma 2016; Pöschke, Fortmann, and Schulte 2017)

$$P = \frac{1}{2} C_p(\lambda, \beta) \lambda \rho \pi R^2 V^3 \tag{1.1}$$

with

- β the blade pitch angle;
- R the radius of the blades;
- ρ the air density; at a temperature of $15°C$ and an atmospheric pressure of 1.0132 bar, the air density is approximately equal to 1.205 kg/m^3;
- V the wind speed;
- λ the tip speed ratio (TSR) being the ratio between the rotation speed of the rotor Ω_r and the wind speed V, and reading as

$$\lambda = \frac{\Omega_r}{V} R. \tag{1.2}$$

The power coefficient C_p characterizes the efficiency of the conversion of wind energy into mechanical energy; such coefficient can be obtained either by real-world experiments or by using accurate simulations. Then, it can be described by different approaches, as look-up tables (Odgaard, Stoustrup, and Kinnaert 2013) (see Figure 1.6) or fitted to a polynomial (Raach et al. 2014) by the following expression

$$\begin{aligned} C_p &= c_1(c_2\xi - c_3\beta - c_4)e^{c_5\xi} \\ \xi &= \frac{1}{\lambda + 0.08\beta} - \frac{0.035}{\beta^3 + 1} \end{aligned} \tag{1.3}$$

with $c_1 - c_5$ the C_p curve fitting coefficients (Guenoune et al. 2017). Therefore, C_p is not well-known and introduces uncertainties to the model.

Figure 1.6 displays the power coefficient C_p versus the TSR λ, for a given blade pitch angle β. It is then strongly influenced by the wind since λ is a function of V. **Then, from** (1.1)**, the power of**

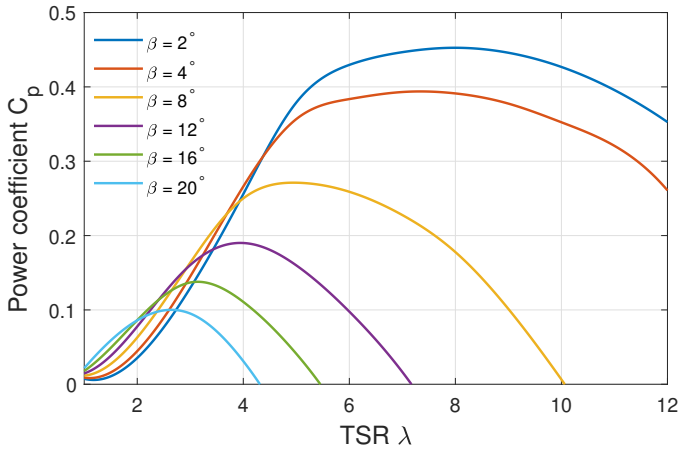

Figure 1.6 – Power coefficient C_p versus the tip-speed ratio λ, for different blade pitch angle β.

the turbine for different wind speeds can be adjusted thanks to the blade pitch angle β.

In addition, wind fluctuations induce torque fluctuations, increasing the fatigue loads on the drive shaft and also affecting the quality of the produced power produced. So, there is a real interest in designing variable speed wind turbines, to adapt their rotation speeds to wind variations in order to obtain the most appropriate C_p value and therefore to optimize the power output in different operating regions (for definition of regions, see previous chapter). The aerodynamic torque developed by the turbine blades is defined by (Guenoune et al. 2017; Huang, F. Li, and Jin 2015)

$$\Gamma_a = \frac{1}{2}\frac{C_p(\lambda,\beta)}{\lambda}\rho\pi R^3 V^2. \tag{1.4}$$

1.2.3 Drive train system

The purpose of the drive train is to transmit wind power and mechanical torque from the turbine to the electric generator (Burton, Sharpe, and Jenkins 2001). There are different types of drive train models, depending on the number of the mass, such as six-mass, three-mass and two-mass models (Muyeen et al. 2007). Among those models, the two-mass model has been widely used in the literature (Novak, Jovik, and Schmidtbauer 1994; Beltran, Ahmed-Ali, and Benbouzid 2008; Abo-Khalil et al. 2019). The complexity of the two-mass model is reduced, but this mdoel is sufficient for characterizing the dynamics of the drive train (McFadden and Basu 2016).

Figure 1.7 illustrates a two-mass drive train model. This model consists in the following elements: two mass with rotational inertia J_r and J_g representing the inertia of the mechanical part (blades, tower and hub) and electrical part (generator rotor) respectively, a low speed shaft (LSS) modeled by a torsional spring and a torsional damper, a rigid high speed shaft (HSS), and finally a gear box

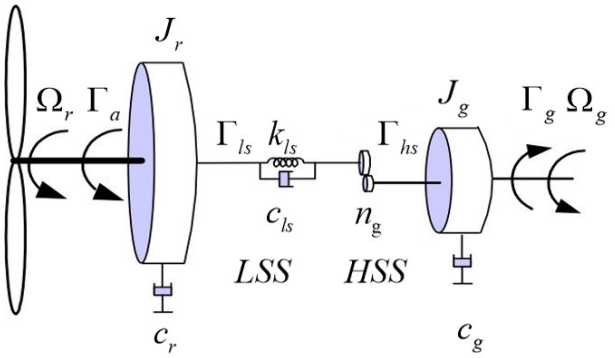

Figure 1.7 – Two-mass drive train model with a gear box (adapted from (Abo-Khalil et al. 2019)).

connecting the two parts, mechanical one (turbine) and electrical one (generator). The mathematical representation of such model is given by

$$\begin{aligned} J_r\dot{\Omega}_r &= \Gamma_a - c_r\Omega_r - \Gamma_{ls} \\ J_g\dot{\Omega}_g &= \Gamma_{hs} - c_g\Omega_g - \Gamma_g \\ \dot{\Gamma}_{ls} &= k_{ls}(\Omega_r - \Omega_g) - c_{ls}(\dot{\Omega}_r - \dot{\Omega}_g) \end{aligned} \tag{1.5}$$

with

- Ω_r the rotor speed;
- Ω_g the electric generator speed;
- n_g the gear box speed-up ratio;
- Γ_a and Γ_{ls} the aerodynamic torque generated by the wind and the LSS torque, respectively;
- Γ_g and Γ_{hs} the generator torque and the HSS torque, respectively;
- c_r, c_g and c_{ls} the damping coefficients of the turbine, generator and shaft, respectively;
- k_{ls} the stiffness coefficient of the LSS.

For simplicity, assume that the rotor is perfectly rigid. So, ignoring the shaft friction (see Figure 1.8), the dynamics of the drive train reads as

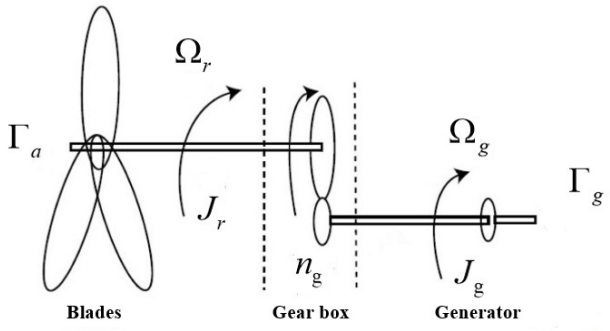

Figure 1.8 – Reduced wind turbine drive train with a gear box (Betti et al. 2013).

$$J\dot{\Omega}_r = \Gamma_a - n_g\Gamma_g \tag{1.6}$$

with J the total inertia of the drive train system. The relation between the total inertia J, and both the rotational inertia J_r and J_g reads as

$$J = n_g^2 J_g + J_r. \tag{1.7}$$

1.2.4 Hydrodynamics

Different from the fixed-bottom wind turbine, due to the presence of a floating platform, additional 6 DOFs (platform horizontal surge, horizontal sway, vertical heave translation and platform roll, pitch, yaw rotation - Figure 1.2) must be considered for the floating wind turbines. These 6 DOFs are infected by the hydrodynamics forces caused by waves, mooring system, and by the aerodynamic forces caused by the wind. Of course, all these factors have a great influence on translations and rotations of the platform. Additionally, in the offshore environment, the dynamics of the platform are highly nonlinear and coupled with the aerodynamics of the turbine system; it is clearly a very complex task to model the hydrodynamics in control design context (Jason M Jonkman, M. L. Buhl Jr, et al. 2005; Y. Shi et al. 2017; Cho 2020). Therefore, specific models for FWT are required in a reduced scale and will be introduced in the next section.

1.3 Linearized model

In the previous subsection, it has been concluded that the blade pitch angle affects the aerodynamic torque Γ_a and thereby, control the rotor speed Ω_r and the power output. However, the dynamics between the floating platform and the blade pitch angle are not obvious; namely, from the control design point of view, the models of the platform (G et al. 2012; Sandner et al. 2012) in the literature are not usable. Therefore, in order to simplify the design process of the controller, linear models

have been usually considered for a reduced number of DOFs.

Linear models used in this work are obtained by the FAST software [2] (B. Jonkman and J. Jonkman 2016). FAST code contains complex and precise wind turbine nonlinear models; such nonlinear models are used as simulation objects that provide accurate aerodynamic and structure responses to the wind, wave, blade pitch... Nevertheless, on the other hand, due to the complexity of the models, from a control point-of-view, such models can not be used for the control design. To this end, FAST has the function of generating linearized representations of wind turbine; then, linear state-space models can be extracted from the FAST and can be used as the "plant" for control design and analysis (Jason M Jonkman, M. L. Buhl Jr, et al. 2005).

The linear model carried out from FAST depends on the considered operating point of the wind turbine. At a specific operating point that depends on the wind speed and the rotor speed, a set of values of the wind turbine system are determined, for example: system DOFs displacements, velocities and accelerations, blade pitch angle .... Once the wind turbine is operating in a steady condition, the operating point values are periodic with respect to the rotor azimuth angle (see Figure 1.5). This periodicity is driven by aerodynamic loads, which depend on the rotor azimuth angle in the presence of prescribed shaft tilt, wind shear, yaw error, or tower shadow. Gravitational loads also drive the periodic behavior when there is a prescribed shaft tilt or appreciable deflection of the tower due to thrust loading (Jason M Jonkman, M. L. Buhl Jr, et al. 2005). Then, for a given operating point, FAST generates a periodic state-space model with a period equal to the time of one rotor revolution. Then, around the operating conditions (x_{op}, u_{op}, δ_{op}), the model reads as

$$\dot{x} \quad = \quad A(\psi) \cdot x + B(\psi) \cdot u + B_d(\psi) \cdot \delta \tag{1.8}$$

where

- $x = \begin{bmatrix} q \\ \dot{q} \end{bmatrix}$ denotes the state vector, $x \in \mathbb{R}^N$, q being the DOFs of the wind turbine system (e.g. rotor azimuth, blade deflections, platform rotations...). The dimension of q and $\dot{q}$ depends on the DOFs enabled in FAST (that is a user's choice);

- u is the control input. For a CBP (see previous chapter) controller, $u = \beta_{col}$ with β_{col} the collective blade pitch angle. For a IBP (see previous chapter) controller, $u = [\beta_1 \ \beta_2 \ \beta_3]^T$ is the control input vector with β_1, β_2 and β_3 the pitch angles of the three blades;

- $A(\psi)$ is the state matrix ($N \times N$), and is periodic with respect to the rotor azimuth angle ψ;

2. A well-known open source software for wind turbine research; it will be introduced in Section 1.4.

- $B(\psi)$ is the input matrix ($N \times 3$), and is periodic with respect to ψ;
- $B_d(\psi)$ is the wind input disturbance matrix ($N \times 1$), and is periodic with respect to ψ;
- δ is the wind disturbance input;
- x_{op}, u_{op} and δ_{op} are the value of the states, inputs and wind speed at the operating point, respectively.

The elements of $A(\psi)$, $B(\psi)$ and $B_d(\psi)$ depend on the properties of the system, such as stiffness and damping. As previously mentioned, these matrices are periodic with respect to the rotor azimuth ψ that induces a periodic model (1.8). In order to simplify the control design, a linear time-invariant model can be derived by averaging system (1.8) with respect to ψ. Notice that the periodic models can be averaged when the system states are located in non-rotating frames, such as the platform frame and the tower base frame (see Figures 1.2 and 1.3).

In the sequel, the azimuth-average model will be used for design of CBP control. However, for the IBP control, the dynamics of each blade are in the reference rotating frame (see Figure 1.4) located in each blade respectively; so, the periodic information on the rotating frame is lost while averaging. Therefore, multi-blade coordinate (MBC) transformation (G. Bir 2008; Karl Stol et al. 2009; Hazim Namik and Karl Stol 2010) is used in order to keep the periodic information before averaging. This class of solution will be detailed in Chapter 4.

1.3.1 Reduced state-space model

The FAST nonlinear floating wind turbine models can have huge number of DOFs, including the blade flap-wise/edge-wise bending mode, the tower fore-aft/side-to-side bending-mode, the platform rotation and translation... In the present work, in order to simplify the control design, a reduced linear model is used with only 2 DOFs, that are the rotor azimuth ψ and the platform pitch rotation φ. This choice has been made because these quantities are related to the control objectives of the study.

Furthermore, as mentioned in the previous subsection, the linearized model (1.8) is periodic with respect to the rotor azimuth angle ψ. Since the two DOFs chosen are in the non-rotating frame of reference, the periodic model can be azimuth averaged, in order to get a linear time-invariant one, reading as

$$\dot{x} = A_{Avg} \cdot x + B_{Avg} \cdot u + B_{dAvg} \cdot \delta \tag{1.9}$$

where A_{Avg}, B_{Avg} and B_{dAvg} are obtained by averaging $A(\psi)$, $B(\psi)$ and $B_d(\psi)$. In a first time, only CBP approach is considered, so, the control input u is the collective blade pitch angle β_{col}. According to FAST linearization, the column associated with the rotor azimuth state is zero, meaning that this state can effectively be eliminated from the state space model (J. Jonkman 2019). Hence, rotor azimuth ψ is not included, that gives a 3-state vector consisting of

$$x \;=\; \begin{bmatrix} \varphi & \dot{\varphi} & \Omega_r \end{bmatrix}^T$$

with φ the platform pitch angle, $\dot{\varphi}$ the platform pitch angle velocity and $\Omega_r = \dot{\psi}$ the rotor speed.

Notice that model (1.9) is efficient only when the system is close from the considered operating point around which it has been established. Among a large operating domain, A_{Avg}, B_{Avg} and B_{dAvg} obtained for a fixed operating point can not accurately represent the system dynamics. Therefore, in order to ensure the accuracy of the linearized system, many systems (1.9) should be carried out at different operating points. For example, when the considered floating wind turbine is operating at a wind speed equals to $18m/s$ and rotor speed equals to its rated value $\Omega_{r0} = 12.1\ rpm$, one has

$$A_{Avg} = \begin{bmatrix} 0 & 1 & 0 \\ -0.0141 & -0.0405 & -0.0004 \\ -0.0757 & -2.3031 & -0.2304 \end{bmatrix}, B_{Avg} = \begin{bmatrix} 0 \\ -0.0035 \\ -1.1864 \end{bmatrix}, B_{dAvg} \;=\; \begin{bmatrix} 0 \\ 0.0001 \\ 0.0276 \end{bmatrix} \tag{1.10}$$

whereas one gets, for a wind speed equals to $20m/s$ and a rotor speed equals to Ω_{r0}

$$A_{Avg} = \begin{bmatrix} 0 & 1 & 0 \\ -0.0141 & -0.0403 & -0.0006 \\ -0.0679 & -2.5069 & -0.3182 \end{bmatrix}, B_{Avg} = \begin{bmatrix} 0 \\ -0.0035 \\ -1.3856 \end{bmatrix}, B_{dAvg} \;=\; \begin{bmatrix} 0 \\ 0.0001 \\ 0.0030 \end{bmatrix} \tag{1.11}$$

Consequently, due to the wind variations in Region III (11.3 m/s to 25 m/s) and considering a large operating domain, it is reasonable to assume the FWT model as follows

$$\dot{x} \;=\; A_{Avg}(x,t) \cdot x + B_{Avg}(x,t) \cdot u + B_{d_{Avg}}(x,t) \cdot \delta \tag{1.12}$$

with $A_{Avg}(x,t)$, $B_{Avg}(x,t)$ and $B_{dAvg}(x,t)$ the matrices containing the parameters of the reduced two DOFs model in the operating domain, namely, the matrices are varying in the different operating points. It is clear that these matrices are evolving with respect to wind speed (depending on time) and rotor speed (depending on the state variable Ω_r).

Moreover, for the convenience of the following nonlinear control design, by a more general point-of-view, the system (1.12) could be viewed as a particular class of nonlinear systems reading as

$$\dot{x} \quad = \quad f_{wt}(x,t) + g_{wt}(x,t)u \tag{1.13}$$

where

- $f_{wt}(x,t)$ contains the term represented by $A_{Avg}(x,t)\cdot x$ and the term $B_{d_{Avg}}(x,t)\cdot\delta$ containing the uncertainties of the system and the perturbations introduced by wind, waves and other external environments;

- $g_{wt}(x,t) = B_{d_{Avg}}(x,t)$ is the input function.

1.3.2 Comparisons with FAST nonlinear reduced model

In the previous subsection, linearized models are carried out from FAST software around different operating points. In the current subsection, simulations have been made between the linearized model (1.9) and the FAST nonlinear model in order to verify if

- the linear model has similar time response as the FAST model and can be used for the control design;

- the linear model obtained for a given operating point is accurate enough if the system operates away from the operating point.

Consider the model (1.9) obtained for a wind speed equals to 18 m/s with no wave, and a rotor speed equals to its rated value; in this condition, the reduced FWT is described by (1.10). On the other hand, FAST can run a nonlinear model with rotor azimuth and platform pitch enabled as DOFs. Simulations are made on the linear and FAST models respectively, in the two following cases

- **Case 1**: 18 m/s constant wind and without wave (similar conditions as the linearization ones);

- **Case 2**: 20 m/s constant wind and without wave.

Both cases of simulations have similar control input, the collective blade pitch angle β_{col} being fixed at a constant value (the value selected here is the operating point value of blade pitch angle derived from the FAST linearization with wind speed equals to 18 m/s, rotor speed equals to 12.1 rpm). Figure 1.9 shows the responses of platform pitch φ and rotor speed Ω_r obtained by both linearized and FAST models when the wind speed equals to 18 m/s (*e.g.* the system operates at the operating

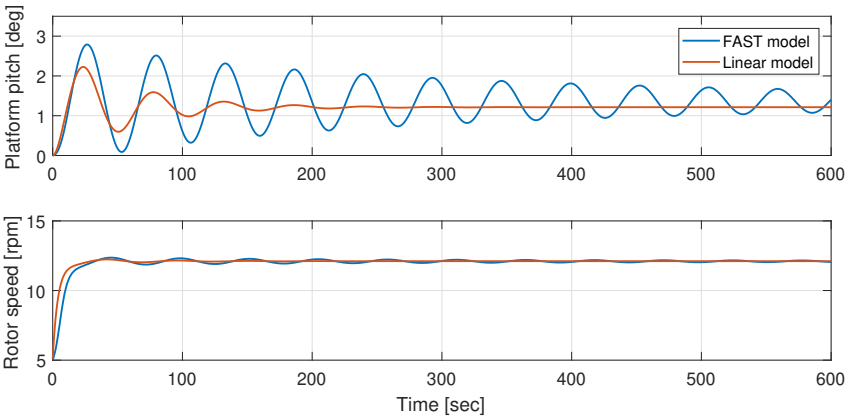

Figure 1.9 – **Case 1.** Platform pitch angle φ (top-deg) and rotor speed Ω_r (bottom-rpm) obtained with both linear and FAST models versus time (sec).

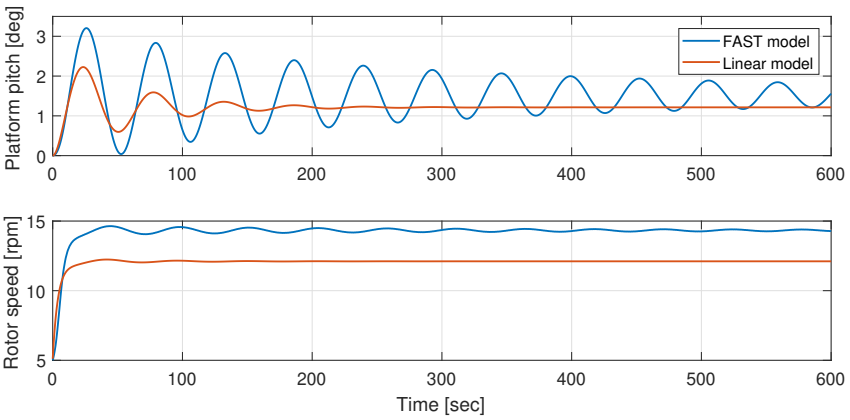

Figure 1.10 – **Case 2.** Platform pitch angle φ (top-deg) and rotor speed Ω_r (bottom-rpm) obtained with both linear and FAST models versus time (sec).

point). It is clear that both the platform pitch angle and rotor speed are finally converging to the same values on the two model. However, there are huge differences in the transient behavior (more oscillating response for FAST model). Figure 1.10 displays the similar simulations but with wind speed equals to 20 m/s that means that for the linearized model, the system works away from the operating point. Obviously, the responses of the platform pitch angle and the rotor speed of the linearized model cannot converge to the same values as the FAST nonlinear model, *e.g.* the system model is no longer accurate if the system operates away from the operating point. As previously, the transient behavior is really different.

Therefore, as declared in the previous subsection, if linear control approaches are used, it is necessary to linearize the nonlinear model at different operating points. However, as previously viewed, dynamic behavior is not repeated by an accurate way. In this thesis, it is exactly the way that one does not want because it makes the control design much more complex and probably less efficient. Indeed, it means "one operating point = one controller tuning". It is the reason why another way will be used: control design based on nonlinear uncertain system.

1.4 Simulation set-up and performance analysis tools

1.4.1 FAST software

FAST (Fatigue, Aerodynamics, Structures and Turbulence) is an open source software developed by National Renewable Energy Laboratory (NREL) (Jason M Jonkman, M. L. Buhl Jr, et al. 2005) and can be used to analyse the structural dynamics of wind turbine systems. FAST is using models of the tower, blades and drive-train as flexible elements and is using bending mode shapes for the analysis. Each blade has two flap-wise and one edgewise bending modes. The tower has two fore-aft and two side-side bending modes. The drive-train flexibility is modelled through a linear spring and a damper for the low speed shaft. The remaining elements of the wind turbine (nacelle and hub) are modelled as rigid bodies. The fidelity of the model can be set by selecting which DOFs are to be enabled or disabled (there are 24 DOFs in FAST model).

With the development of floating wind turbines, additional dynamics introduced by floating offshore environment is considered in the FAST code; indeed, the hydrodynamics module and mooring lines module used for floating platform dynamics are developed in (J. Jonkman and Sclavounos 2006). As shown in Figure 1.11, the overall FAST floating wind system is composed by the coupled aero-dynamics, hydrodynamics, turbine dynamics and mooring line dynamics.

As detailed in subsection 1.3, FAST also has the capability to provide a linearize model of the FWT

at a specific operating point.

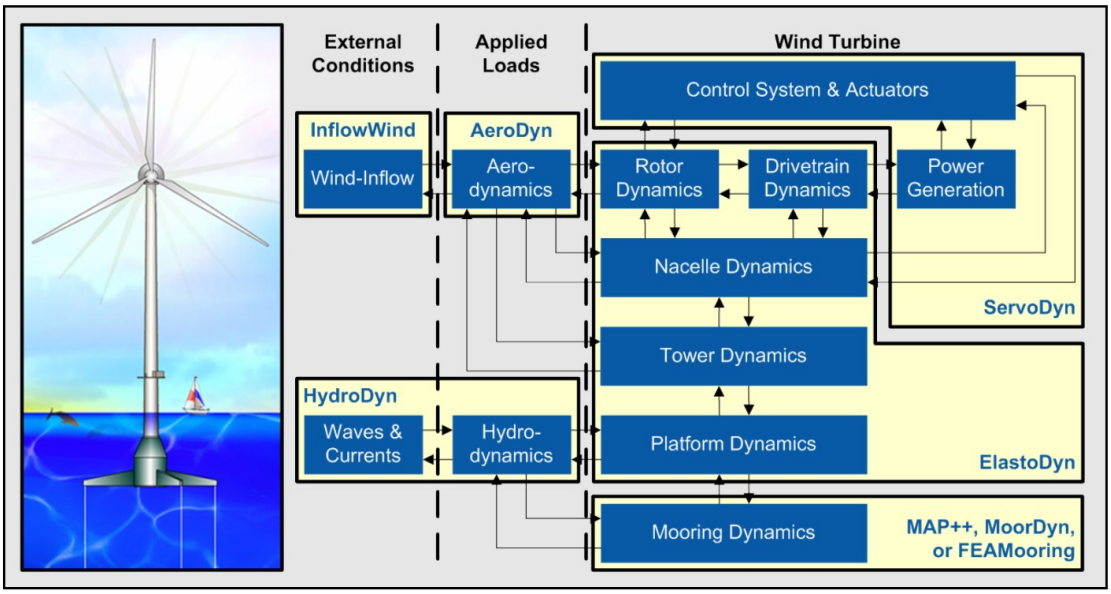

Figure 1.11 – FAST structure for floating wind systems (B. Jonkman and J. Jonkman 2016).

The control system can be integrated in the FAST simulation environment. The wind turbine actuators (blade pitch, generator torque, yaw drive and high-speed shaft brake) can be controlled by a dynamic link library (DLL) file or by interfacing with SIMULINK (Hazim Namik 2012). As a well-known simulation tool for control design, SIMULINK allows to develop the control scheme with high flexibly. The FAST software has the ability to be linked with SIMULINK through a s-function: this offers a convenient way to design control in the SIMULINK environment while using the nonlinear model described by FAST. Figure 1.12 displays the structure of control/system co-simulator: it is composed of FAST model (green box) that contains s-function with equations of motions and, in SIMULINK, the controllers providing the adapted signals.

1.4.2 5MW spar-buoy floating wind turbine model

In this study, the "NREL offshore 5MW OC3-Hywind" floating wind turbine model from the FAST software will be used for all the simulations. This model is based on the NREL offshore 5MW wind turbine (J. Jonkman 2010; J. Jonkman, Butterfield, et al. 2009), which is a well-known turbine and widely used in the research field of wind turbine, the main properties of this wind turbine being displayed in Table 1.1.
The platform applied to this FWT model is the spar-buoy concept and has been developed by Statoil of Norway on the Offshore Code Comparison Collaboration (OC3) project (Passon et al.

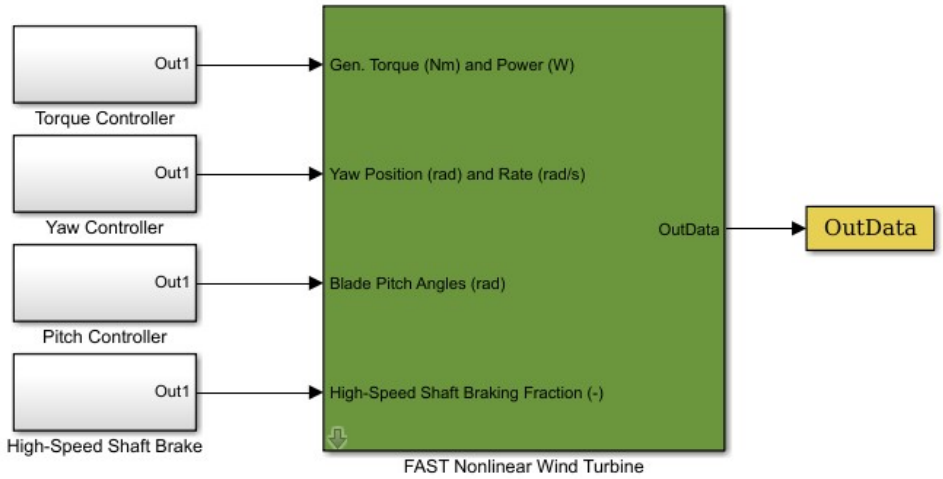

Figure 1.12 – Model and control scheme using FAST code (green box) in MATLAB/SIMULINK environment.

Description	Value
Cut-in, rated, cut-out wind speed	3 m/s, 11.4 m/s, 25 m/s
Rotor diameter	126 m
Hub diameter	3 m
Hub height	90 m
Rated power	5 MW
Rated rotor speed	12.1 rpm
Rated generator speed	1173.7 rpm
Rated generator torque	43,093.55 N·m
Minimum blade pitch setting	0 °
Maximum blade pitch setting	90 °
Maximum blade pitch rate	8 °/s

Table 1.1 – Properties of the NREL 5MW wind turbine (J. Jonkman, Butterfield, et al. 2009).

2007); it is known as "Hywind". Such concept has been chosen because of the simplicity in design, good stability and comparatively easy to implement in practice. Notice that the original Hywind spar-buoy is equipped by a 2.3-MW wind turbine. In order to support the NREL 5MW wind turbine, Jason Jonkman of NREL has adapted slightly the properties of the floating structure. Table 1.2 summarizes the main properties of the platform. Figure 1.13 illustrated the NREL 5MW OC3-Hywind floating wind turbine and the main dimensions of the spar platform.

Parameters	Value
Depth to platform base below still water level (SWL)	120 m
Elevation to platform top above SWL	10 m
Platform diameter above taper	6.5 m
Platform diameter below taper	9.4 m
Platform mass	7,466,330 kg

Table 1.2 – Properties of OC3-Hywind spar-buoy platform (J. Jonkman 2010).

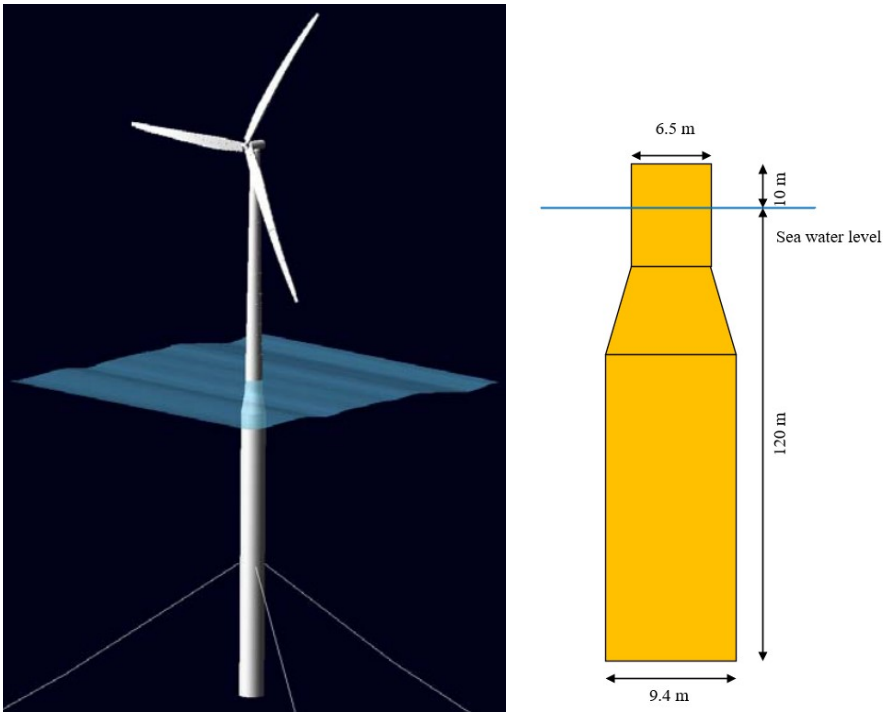

Figure 1.13 – **Left**. Illustrations NREL 5MW OC3-Hywind floating wind turbine (J. Jonkman 2010). **Right.** Main dimensions of OC3-Hywind spar-buoy platform.

1.4.3 Performance indicators

Different kinds of performance indicators are used in the sequel to precisely compare the controllers, it is the main way to have accurate comparison between the proposed control approaches. The objective being the evaluation of the controllers efficiency, the idea consists in evaluating the amount of produced power, the global behaviour of the FWT (motions, structure loads,...).

The first indicators are the root mean squares (RMS) of the power output, rotations and motions of the turbine and floating platform respectively. These RMS values allow to check the quality of the tracking (power/rotation speed) and the limited motions of the FWT.

The second indicators are the fatigue damage equivalent loads (DEL) that are used to evaluate the lifetime of the key components; such indicators are calculated by the post processing code Mlife (Gerber and M. Buhl Jr 2012).

Finally, the variation (VAR) of the blade pitch angle evaluates the activity of the blade pitch actuator: intensive action on blade pitch angle implies high energy consumption and could also reduced the lifetime of the actuator. Recall that VAR of a function Y (B. Wang et al. 2014) reads as

$$\mathrm{VAR}[p,q] = \sum_{i=p}^{q} |Y_{i+1} - Y_i|, \tag{1.14}$$

with $[p, q]$ the interval of sampled system output.

To summarize, the performance indicators are divided into the following categories:
Power, rotor speed regulation and motions of floating platform. The smaller the values, the better the performances.

- RMS of generator power error with respect to rated power (5 MW);
- RMS of rotor speed error with respect to the rated rotor speed (12.1 rpm);
- RMS of platform roll and its rate;
- RMS of platform pitch and its rate;
- RMS of platform yaw and its rate;

Fatigue loads of key components. The lower the value means the lower fatigue load of corresponding component.

- DEL of tower base (TB) fore-aft moment;
- DEL of tower base (TB) side-to-side moment;
- DEL of tower base (TB) torsional moment;

- DEL of blade root (BR) flap-wise moments;
- DEL of blade root (BR) edge-wise moments;
- DEL of fair-lead force (FF) of mooring lines;
- DEL of anchor force (AF) of 3 mooring lines.

Activity of blade pitch actuator. A high value implies its frequent use and is a key-indicator in order to detect, for example, chattering when sliding mode based control law is used.

- VAR of blade pitch angle.

1.5 Conclusions

This chapter has described the modeling of a FWT system, the simulation system and the analysis of performances. Firstly, the coordinate system is established. Physical models of power capture and drive train system are introduced. Then, a brief explanation of hydrodynamics of the floating structure is given. For the control design point of view, the linearized model of FWT is introduced and compared with the FAST nonlinear model. Finally, FAST software used in the sequel for the simulations of a 5 MW spar-buoy FWT is introduced, and performance indicators are defined.